Stark mapping of H_2 Rydberg states in the strong-field regime with dynamical resolution

W. L. Glab and K. Qin
Department of Physics, Texas Tech University, Lubbock, Texas 79409
(Received 13 May 1993)

We have acquired spectra of high Rydberg states of molecular hydrogen in a static external field, in the energy region from below the energy at which field ionization becomes classically possible (E_c) to well above this energy. Simultaneous spectra of ionization and dissociation were acquired, thereby allowing direct information on the excited-state decay dynamics to be obtained. We have found that states with energies below E_c undergo field-induced predissociation, while states with energies well above E_c decay predominantly by field ionization. Field ionization and dissociation compete effectively as decay channels for states with energies in a restricted region just above E_c. Comparison of our ionization spectra to the results of a single-channel quantum-defect theory Stark calculation shows quantitative agreement except near curve crossings, indicating that inclusion of different core rotational state channels will be required to properly account for coupling between the Stark states. Several states in the spectra undergo pronounced changes in their dynamical properties over a narrow range of field values, which we interpret as being due to interference cancellation of the ionization rates for these states.

PACS number(s): 33.55.Be, 33.80.Rv

INTRODUCTION

The Stark effect on Rydberg states of diatomic molecules has been of considerable interest recently. While the development of the quantum-defect theory (QDT)-Stark theory for complex atomic systems has led to good agreement between theory and experiment for several atomic systems [1], extension of this theoretical framework to molecular systems is still in its infancy. Only one application of this theory to a molecular system, H_2, has been reported [2]. However, this work did not address a fundamental difference between atomic and molecular systems: the presence in the molecular case of the decay channel of dissociation. Electric-field ionization was also not considered. In a molecule, dissociation can compete with electric-field ionization in determining the fate of the Rydberg molecules. This competition has not been explored experimentally in a systematic way. Only one previous study has examined the Stark effect on molecular Rydberg states with resolution of the decay channels of the excited states [3]; this study by one of the authors presented ionization and dissociation spectra in the region near E_c, the energy at which classical escape of the excited electron becomes possible, for a single value of the electric field. The region of energy around and above E_c can be viewed as the lower limit of the strong-field regime, in which perturbation theory becomes inapplicable to the system of molecule and external field.

Only a few studies of the Stark effect in molecules in a static field, near and above E_c, have been reported. In addition to the study of H_2 by one of the authors, the formation of hydrogenic Stark manifolds in Na_2 has been observed [4]. Forced autoionization and electric-field effects on rotational autoionization in Li_2 have been studied [5,6]. The Stark effect on vibrationally autoionizing states of H_2 has been reported [7,8]. A very recent work by the authors examined the formation of Stark manifolds, rotational interactions between Stark states, and field-induced predissociation in Rydberg states of H_2 converging to the ground vibrational state of the ion core [9]. We have also observed competition between vibrational autoionization and dissociation in Rydberg states of H_2 in the weak-field regime (below the Inglis-Teller limit at which n mixing becomes significant) [8]. Another very recent paper studied the lifetimes of H_3 Rydberg states in an electric field [10]. Several works have appeared which discuss the decay dynamics of high-principal-quantum-number molecular Rydberg states in an electric field, in the context of zero kinetic energy photoelectron spectroscopy (ZEKE-PES) [11,12].

In order to understand the molecular Stark effect as fully as possible, it is desirable to experimentally generate Stark maps of spectra versus electric-field strength which separate the yields of molecular ions (due to field ionization) and the atomic products of dissociation. Such spectra would enable a detailed comparison of experiment to an extension of QDT-Stark theory which includes the spectroscopic and dynamic effects of the rotational and vibrational structure of the molecular core.

Molecular hydrogen is the ideal system for studies of this kind, since its zero-field properties are well known, the large rotational and vibrational spacings of its ionic core lead to an open spectral structure, and its high-np singlet Rydberg states are relatively stable against predissociation [13] compared to those of many other diatomic molecules.

We have generated Stark maps of molecular hydrogen with resolution of the two dominant decay channels, dissociation and field ionization, covering field strengths from about 3.2 to about 5.3 kV/cm, for state energies ranging from below E_c (the energy at which the excited electron can escape classically) to well above E_c. The general behavior of the excited-state dynamics in this en-

ergy region is found to be in agreement with that inferred in a previous study which reported spectra for a single field value [3]: dissociation dominates for energies less than E_c, ionization dominates for energies well above E_c, and the two processes compete effectively in an energy region just above E_c. Many of the observed states can be identified by comparison to the results of fourth-order perturbation theory calculations. In several instances, resonances are observed to appear strongly in dissociation over a narrow range of field strengths. We believe that this behavior is due to localized reductions in the ionization rate of some Stark states caused by interference-induced cancellation of the rate near curve crossings. A comparison of our results to a single-channel QDT-Stark calculation shows some quantitative agreement, but indicates that in order to achieve agreement near curve crossings the interactions between rotational states of the ionic core must be taken into account.

EXPERIMENT

The experimental arrangement which we use is very similar to that described in the earlier work of one of the authors [13]. Molecular hydrogen, in a molecular beam formed from a pulsed valve, is excited from the ground rovibrational state of the ground electronic state ($X\,^1\Sigma_g$ $v''=0$, $N''=0$, where N denotes the quantum number for the total angular momentum exclusive of spin) to the $v'=0$, $N'=0$ state of the $E\,^1\Sigma_g$ state by the absorption of two photons at 202 nm. The 202-nm light is produced by frequency tripling an Nd^{3+}:YAG pumped pulsed dye laser in potassium dihydrogen phosphate (KDP) and beta barium borate (BBO) crystals [14]. High-lying Rydberg states in the region of the first ionization limit are then excited by absorption of another photon from a tunable, narrow-band pulsed dye laser operating near 400 nm. This laser has a bandwidth of about 0.03 cm^{-1}, and is polarized either along the electric field, so that we produce Rydberg states with a projection of total angular momentum equal to zero ($m_J=0$), or perpendicular to the field, so that we excite states with $m_J=1$. The excitation occurs between two field plates separated by 0.93 cm, across which a voltage is applied to create a Stark field and extract laser-produced ions. Fields of up to 5350 V/cm can be produced, with a uniformity within the laser beam volume of better than 0.5%. Field nonuniformity is the primary cause of broadening in our experimental spectra. Our field calibration was initially believed to be accurate at a 1% level.

Excited hydrogen atoms in the $n=2$ state, produced by dissociation of the excited molecules, are ionized through $1+1$ resonant multiphoton ionization using light from a third tunable dye laser at 656 nm (the wavelength of the Balmer α transition) to excite the $n=2\rightarrow n=3$ transition, and 532-nm light from the YAG laser to ionize the excited atoms. These laser beams are delayed from the pulse which excites the Rydberg states by a few nanoseconds, and result in nearly complete ionization of the excited dissociation products. The small delay between the excitation and decay product detection lasers leads to some temporal overlap between the pulses. The 656-nm light easily saturates the $n=2\rightarrow n=3$ transition; once in the $n=3$ state, the excited atoms are rapidly ionized. This arrangement ensures that the efficiency with which dissociation is detected does not significantly depend on the $n=2$ Stark state of the atomic product. The atomic and molecular ions are detected separately after passage through a 50-cm-long flight tube. The ion signals, as well as an optogalvanic calibration spectrum of uranium [15], are acquired by a personal computer. Signals from ten laser shots are averaged at each laser wavelength. Thus, as the laser which excites the Rydberg states is tuned, simultaneous spectra of ionization and dissociation are acquired. Stark maps are produced by scanning the blue laser over several hundred wave numbers of energy at a number of electric-field strengths (separated by about 50 V/cm) ranging from about 3.2 to 5.3 kV/cm.

THEORETICAL BACKGROUND

A nonhydrogenic atomic or molecular system has one or more quantum defects which are nonzero, leading to fundamental differences between the Stark effect of atomic hydrogen and that of all other species. Penetrating states (those with low values of the orbital angular momentum quantum number l) typically have nonzero quantum defects in a complex system: in an atom, states with different values of l and J (the total angular momentum quantum number) will each have a different value for the quantum defect, while in a molecular system the quantum defect will also depend on the core rotation quantum number R (assuming Hund's case d coupling, as is appropriate for highly excited states).

At fields which are relatively weak [$F<\delta/(n^5)$, where δ is the quantum defect of the penetrating state in question], the nonpenetrating states will be mixed by the field to form an incomplete hydrogenic Stark manifold of linearly shifting states, while the penetrating state will experience a quadratic Stark shift. As the field is increased, the penetrating state will be fully mixed with the manifold resulting in a nearly hydrogenic pattern of linearly shifting Stark states. In a molecular system, electronic-rotational coupling also leads to interactions between Stark manifolds arising from different core rotational states. The Stark effect in these regimes of field strength can be modeled accurately through diagonalization of a limited basis Stark Hamiltonian matrix which includes rotational interactions in the molecular case [9].

As the field is increased past the Inglis-Teller limit ($F>1/3n^5$), manifolds of different n begin to interpenetrate. In a complex system, the Stark components of different manifolds undergo avoided crossings whose size is determined by the nonzero quantum defects of the system [16]. The Stark structure in this n-mixing regime can be calculated by diagonalization of a Stark Hamiltonian which includes couplings due to the nonhydrogenic core [16], or by QDT-Stark calculations [17] which will be discussed later in this paper.

Field ionization becomes possible for energies above $E_c=-2\sqrt{F}$ (in atomic units). In this regime, as well as

in the n-mixing regime, n is no longer a good quantum number, and the states should be labeled with their energy E, parabolic quantum number n_1, and azimuthal quantum number m. However, for states which do not ionize too rapidly, we can still retain n as a state designation. The quantum numbers n and m are related to the parabolic quantum numbers n_1 and n_2 through the expression $n=n_1+n_2+|m|+1$, where m is taken to be a positive number (the cylindrical symmetry of the combined potential leads to a twofold degeneracy between states with the same value of $|m|$). States with values of $n_1>(n-|m|-1)/2$ are blueshifted by the field, while states with $n_1<(n-|m|-1)/2$ are redshifted. In general, states in a given energy region that are the most blueshifted ($n_1\sim n-|m|-1$) are most stable against field ionization, while those which are the most redshifted ($n_1=0$) have the highest field ionization rates. In this region of field and energy the field effect is not weak, and one would anticipate that perturbation theory would fail to predict the state energies accurately. However, the energies of states which have relatively low ionization rates can be predicted accurately using the results of a fourth-order perturbation theory calculation [18]. Analytic formulas have been presented for the ionization rates of hydrogenic Stark states [19], but more accurate results are obtained through calculating photoionization cross sections by numerical integration of the Schrödinger equation in parabolic coordinates [20] (for atomic hydrogen) or QDT-Stark theory (for complex atoms) [1].

In a nonhydrogenic system, the ionization rates of most of the field-ionizing states are mostly due not to purely hydrogenic escape over the lowered Coulomb+Stark barrier, but rather to core-induced couplings between the quasidiscrete Stark states and other Stark states which have broadened into ionization continua. Thus the ionization widths are determined by the quantum defects of the system in question, and can be determined using QDT-Stark theory. In this theoretical approach, space is divided into several regions: the core region in which the effect of the external field is negligible and the potential nonhydrogenic, a region outside of the core in which both Coulombic and Stark-parabolic wave functions are equally valid, and an outer region in which the Stark field dominates. The effect of the core is embodied in the phase shifts of the various Coulombic wave functions outside of the core, due to the nonhydrogenic part of the core potential. The long-distance behavior of the wave function is determined by application of the appropriate boundary conditions on the parabolic wave functions appropriate to the Stark effect. The wave function for all of space outside of the core can then be found utilizing a frame transformation between the spherical and parabolic bases to connect the inner and outer regions. Photoionization cross sections may then be calculated.

This theoretical approach has proven to be very successful for the study of complex atomic systems. For systems with a closed-shell ionic core, such as alkali-metal atoms, the core lacks low-energy structure and only a single core state participates in the observed phenomena. Such atoms may be treated using single-channel QDT-Stark theory (where the term "single-channel" means that only a single *core* channel is important). Open-shell cores have different fine-structure states, each of which has a Rydberg series associated with it. These various Rydberg series can interact either in the absence of or in the presence of a field, mutually perturbing each other. Atoms with such cores must be treated using a multichannel QDT-Stark theory approach which includes multiple core channels, as has been done recently for barium [1].

The extensions of QDT-Stark theory to a molecular system such as hydrogen is certainly possible, but rather involved. Such an extension must account for two new features in a molecule: the presence of new closed and open ionization channels due to the rotational-vibrational structure of the core, and the presence of a different class of channels open to dissociation. The rotational-vibrational structure of the core can be accounted for by including an additional frame transformation from Hund's case (b) to Hund's case (d) coupling, at small distances from the core. The physical results of the presence of these channels are mutual perturbations between states of series which converge to different core states (leading to energy shifts and dynamic effects), and the possibility of predissociation of the Stark states. Inclusion of rotational channels in the case where field ionization is unimportant has already been accomplished [2], as has the inclusion of channels closed to ionization and open to dissociation in the field-free case [20] by the utilization of a generalized quantum-defect theory for the internuclear coordinate in addition to the electronic coordinate. The production of a theoretical model of the molecular Stark effect which includes both rovibrational core channels and dissociative channels is apparently a possible but formidable task.

Earlier studies by the authors have observed predissociation of H_2 Stark states, both in the low-field [8,9] and strong-field [2] regimes. One of these studies has presented evidence that, at least for weak fields, predissociation can be induced into a Stark state by field-induced mixing of states with different dynamical properties [9]. That is, a p state (which is stable against predissociation in the absence of a field) will be mixed with s and d states (which have significant predissociation rates) and acquire an observable predissociative rate. In this model, the predissociation rates of the Stark states is determined by the zero-field predissociation rates of the nonhydrogenic basis states and their degree of admixture into the Stark states. Another possibility which may become important at higher fields is directly field-induced predissociation due to field mixing of excited *ungerade* Rydberg states with *gerade* dissociation continua [22].

Regardless of the specific cause of field-induced predissociation, we would expect that the induced rates would fall off with increasing principal quantum number like $1/n^3$, reflecting the decrease in probability that the excited electron collides with the core. Deviations from this behavior could be caused by indirect predissociation, but such deviations would be localized in energy near predissociated perturbing states. Field ionization rates of Stark states increase rapidly as their energies go above E_c.

These trends lead to the following dynamical behavior of the Stark states near E_c: below E_c the Stark states decay by field-induced predissociation, far above E_c field ionization dominates predissociation since the ionization rates become very large while the dissociation rates drop off, and in a limited region above E_c ionization and predissociation compete effectively in determining the decay of the Stark states. Furthermore, we would expect that in the region of competition dissociation would tend to be the important decay mechanism for those states which are most stable against ionization, the strongly blueshifted states with large values of the parabolic quantum number n_1. These expectations are fully borne out by our experimental results.

Another possible effect of core-induced mixing between Stark states has been studied extensively in atomic systems. This is the phenomenon of interference-induced stabilization against ionization which can occur in a narrow range of field strengths near an avoided crossing [23–25]. The ionization rate of one of the states which is undergoing a crossing can be reduced by orders of magnitude over a range of field of only a few volts/cm. A detailed comparison of experimental results in Na to calculations using a modified QDT-Stark model has been presented, showing excellent agreement between theory and experiment [25]. These reductions in ionization rate are attributable to destructive interference between the amplitudes for ionization through different open parabolic channels.

It is interesting to consider whether such interference phenomena might be observable in a molecule, with its extra degrees of freedom compared to an atom. It should be noted that if such interferences do occur in a region not too far above E_c, they might be more easily seen in a molecule than in an atom, and in an entirely different way. We would expect that when the ionization channel is closed off through cancellation for a particular state, dissociation would become the dominant decay channel. Thus, the most prominent signature of an interference-induced cancellation of the ionization rate for a state would be its appearance in dissociation over a narrow range of field strength near a curve crossing. We have seen such behavior in our Stark maps.

RESULTS AND DISCUSSION

As discussed earlier, the principal results of this work are in the form of Stark maps for each of the important decay channels, ionization and dissociation. Figure 1 shows the Stark map for ionization over an energy range from -500 to -300 cm^{-1} for a number of fields between 3.2 and 5.3 kV/cm, for excitation of the Rydberg states using π-polarized light ($m_J=0$ final states). Figure 2 shows the dissociation spectra for the same range of energy, electric-field strength, and the same polarization. Figures 3 and 4 show the ionization and dissociation spectra, respectively, for the same range of energy and field strength but for σ-polarized light ($m_J=1$ final states).

We now point out some general features of the behavior of the Stark resonances which can be seen in

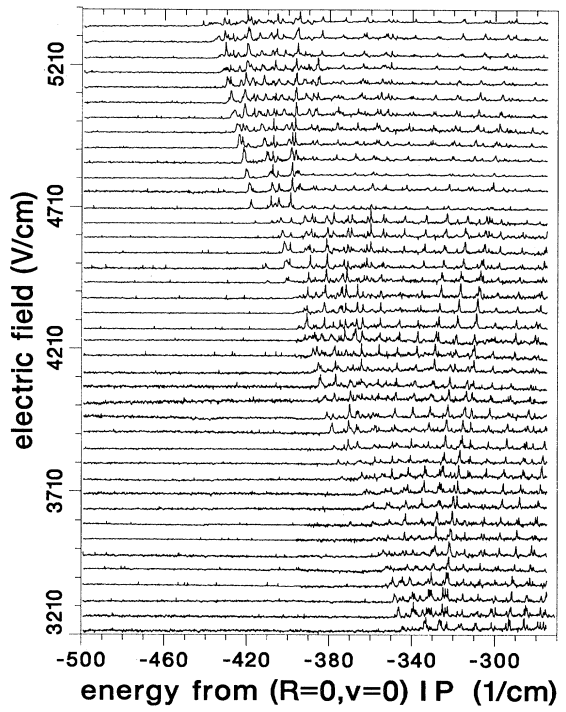

FIG. 1. Stark ionization spectra for π-polarized light. The electric-field strength increases from bottom to top, and the energies are referred to the first ionization limit ($R=0$). IP denotes ionization potential.

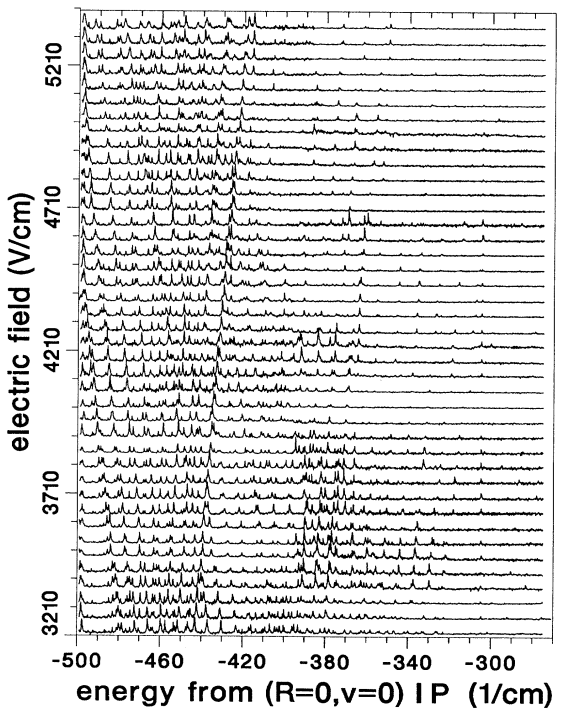

FIG. 2. Stark dissociation spectra acquired simultaneously with the ionization spectra of Fig. 1.

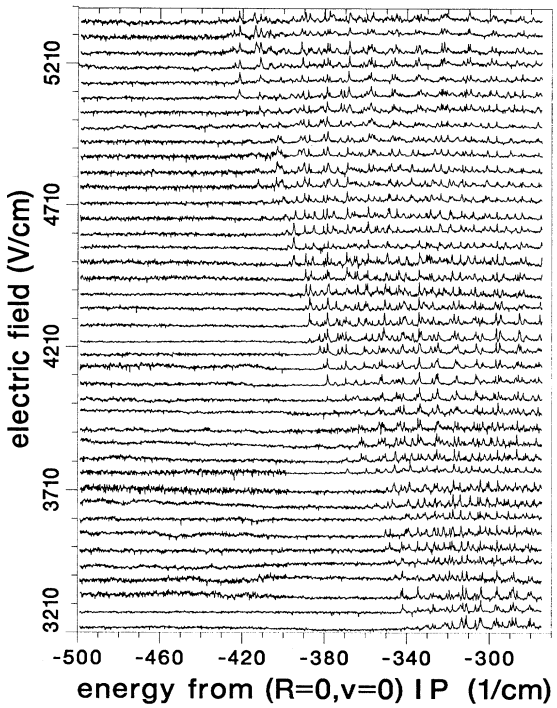

FIG. 3. Stark ionization spectra for σ-polarized light.

these maps. The maps clearly show Stark manifolds originating from zero-field states with different values of the principal quantum number n, with individual Stark states undergoing approximately linear Stark shifts as the manifolds spread out. As the states spread out, they can be seen to undergo a large number of avoided crossings with other Stark states. The separations between Stark states at these avoided crossings reflect the strength of the core-induced couplings between those particular states.

In many cases we can unambiguously identify the Stark resonances by comparing the observed energies of these states with the results of fourth-order perturbation theory calculations. Figure 5 shows a region of the ionization spectra for π-polarized light, along with dotted lines which represent the calculated energies of the Stark states as a function of field strength. Figure 6 shows the dissociation spectra in the same region of field strength and energy. In areas where the Stark spectra are not too congested, the observed and predicted energies match up sufficiently well to allow identification of the states. Several states are designated on the figure, labeled with the quantum numbers n,n_1. The match between calculated and experimental energies is best for blueshifting states, which is to be expected since these are the states with the lowest hydrogenic ionization rates; therefore, perturbation theory would be expected to be accurate for these states. Identification of the states is more difficult in congested regions where core-induced interactions between the states shift their energies from the hydrogenic values considerably.

We turn now to a discussion of the observed decay dy-

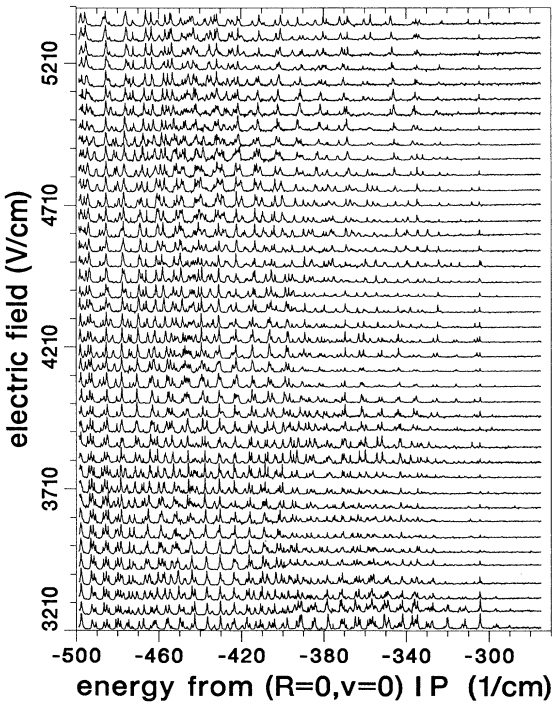

FIG. 4. Stark dissociation spectra for σ-polarized light.

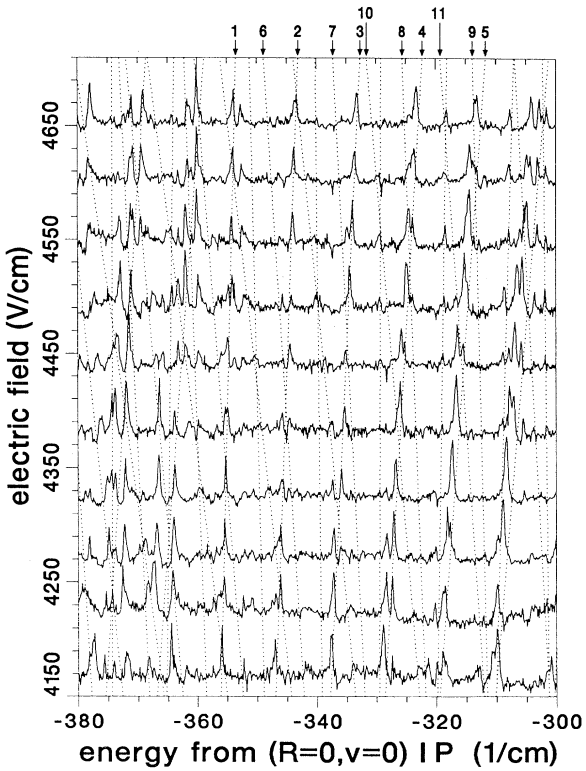

FIG. 5. Expanded plot of the π-polarization ionization spectra of Fig. 1. The dotted lines are the Stark state energies predicted by fourth-order perturbation theory. Some states have been identified; to reduce congestion in the figure, these are labeled by numbers. The identified states are (n,n_1); 1=(17,6); 2=(17,8); 3=(17,10); 4=(17,12); 5=(17,14); 6=(19,−6); 7=(19,−4); 8=(19,−2); 9=(19,0); 10=(20,−7); 11=(20,−5).

namics of the Stark states. In all cases, ionization appears as the state energy rises above E_c. Below E_c, all of the observed states decay by dissociation; with our detection scheme, we are sensitive to rates on the order of 10^8 s^{-1} or greater. The absence of significant broadening in most of the observed resonances below E_c implies that the dissociation rates are generally less than about 10^{10} s^{-1}. Thus our results constrain the possible values for the dissociation rates of the Stark states to this range, and show that all of the Stark states have dissociation rates which are not too different from one another.

In a region above E_c which is about 50 cm^{-1} wide, both the ionization and dissociation spectra show peaks at the many of the same locations. In this region of energy, the decay processes of ionization and dissociation are competing effectively. We cannot determine absolute values of the branching ratio for each state accurately, due to uncertainties in the ionization efficiency of the atomic products and collection efficiencies of the atomic and molecular ion products. However, comparison of the peak heights in each dynamic channel for a given resonance gives a measure of the relative importance of each decay channel for the Stark state. The spectra are generally too congested in this spectral region to pick out individual crossings between states.

At still higher energies, fewer peaks are seen in dissociation than in ionization. This indicates that many of the Stark states have acquired ionization rates larger than $\sim 10^{10}$ s^{-1}; for these states, ionization wins out over dissociation in determining the decay channel of the excited state. Indeed, some Stark states have broadened out to the point of becoming unobservable at these energies. The disappearance of these states from the spectra leads to some simplification, and in this energy range we can pick out some isolated avoided crossings. An example is the crossing of the (19,−6) state [where the state is labeled with (n,n_1)] with the (17,8) state near −345 cm^{-1} at a field strength of about 4.4 kV/cm. The states which still can be observed in dissociation in this region of energy are those which are most strongly blueshifted. It is just these states which would be expected to have relatively small ionization rates on the basis of hydrogenic theory. At energies above those presented in Figs. 1–4 no peaks are seen in dissociation, although structure persists in the ionization spectra. At these higher energies all states have ionization rates considerably greater than their dissociation rates and consequently appear only in ionization.

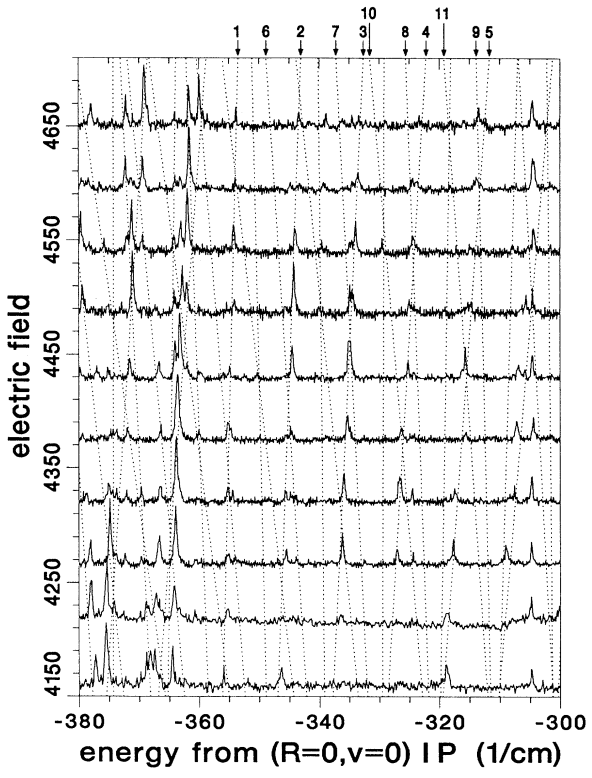

FIG. 6. Expanded plot of the π-polarization dissociation spectra of Fig. 2. State identifications are the same as in Fig. 5.

A minimally complete theory of the Stark effect of H_2 in the region of field and energy which we have considered would include the interaction between several core rotational state channels, as well as field-induced predissociation. Such a theoretical model has not yet been developed. However, it could be argued as follows that a single-channel QDT-Stark calculation might reproduce the general features of the observed spectra. The most important interaction near the first ionization limit between zero-field states which are typically excitable from an $N=0$, even-parity initial state of para-H_2 is the rotational interaction between Rydberg states which converge to the $R=0$ and $R=2$ ionic core states. Since the corresponding ionization limits are separated by 176 cm^{-1}, the $R=2$ states are less affected by the field than the $R=0$ states in a given region of energy; in particular, at 4 kV/cm the $R=2$ states will not be classically field ionized until their energy reaches −211 cm^{-1} relative to the $R=0$ ionization limit. These states will not field ionize in the energy region which we have studied, within our observation time. However, in the region of field strength and energy under consideration in this study the $R=2$ Rydberg states are still strongly split. At 4 kV/cm, the Inglis-Teller limit (at which manifolds of different n interpenetrate) is reached at an energy of −440 cm^{-1} relative to the $R=0$ ionization limit for the $R=2$ Rydberg states. Thus the $R=2$ Stark states are spread over the entire energy region. Each $R=2$ Stark state will interact with each $R=0$ Stark state with a coupling which is reduced significantly from the field-free coupling due to the reduced charge densities of the Stark states near the core compared to the field-free states. By this argument, we might expect that the $R=2$ states would not affect the $R=0$ Stark spectrum much, except in localized regions where avoided crossings between $R=0$ and $R=2$ states occur. If this were true, a single-channel calculation using the known zero-field quantum defects of the $R=0$ series of H_2 might give accurate results for the ionization spectra over many regions. Although such a treatment would not consider dissociation explicitly, one would be able to deduce that all states with sufficiently high ionization rates ($>10^{10}$ s^{-1}) would appear in ionization only,

those with rates small enough ($< 10^8$ s^{-1}) would appear in dissociation only, and that states with intermediate values of the ionization rate would branch significantly into each decay channel.

We have compared the ionization in some restricted regions of energy to the results of a single-channel calculation using the quantum defects $\delta_s = -0.116$ [26], $\delta_p = 0.011$ [13], and $\delta_{l>1} = 0$. We have taken all of the oscillator strength to lie in the excitation of the p-state series, which is reasonable for our case of H_2 since we are exciting from the E, $v = 0$ state, which is almost purely a $2s\sigma$ state. We have convoluted the theoretical spectrum with a 0.5-cm^{-1} full-width Lorentzian profile to approximate the instrument response. A comparison between experiment and theory is shown in Fig. 7 for a theoretical field strength of 4.275 kV/cm and an experimental field strength of 4.32 kV/cm, in an energy region which contains the avoided crossing between the (19,−6) and (17,8) states. This theoretical field strength was selected to give the best agreement between the theoretical and experimental energies, and indicates that our experimental field calibration may be high by about 1.0%. The QDT-Stark calculation reproduces the experimental spectrum over most of the energy region with quantitative agreement, predicting the energies and approximate line strengths well. However, the agreement is not good near curve crossings of the Stark states; in particular, the separation of the (17,10) and (20,−9) states at their avoided crossing near -337 cm^{-1} is underestimated by the theoretical results. The same is true of the crossing between the (19,−10) and (16,15) states near -365 cm^{-1}. It seems to be generally true that the single-channel calculation predicts smaller avoidances at crossings than are observed in the experimental spectra. Also, additional structure which is not present in the results of the single-channel theoretical calculation can be seen for some energies and field strengths. These discrepancies indicate that the single-channel approach seriously underestimates the core-induced coupling between the Stark states. It is evident that the excited core rotational channels must be explicitly included through a treatment, to give correct values for the core-induced coupling. It could also be that other approximations which appear in the theoretical treatment, such as the use of WKB techniques for the calculation of decay rates and ignoring the dependence of the quantum defects on internuclear separation, may contribute to the disagreement with experiment.

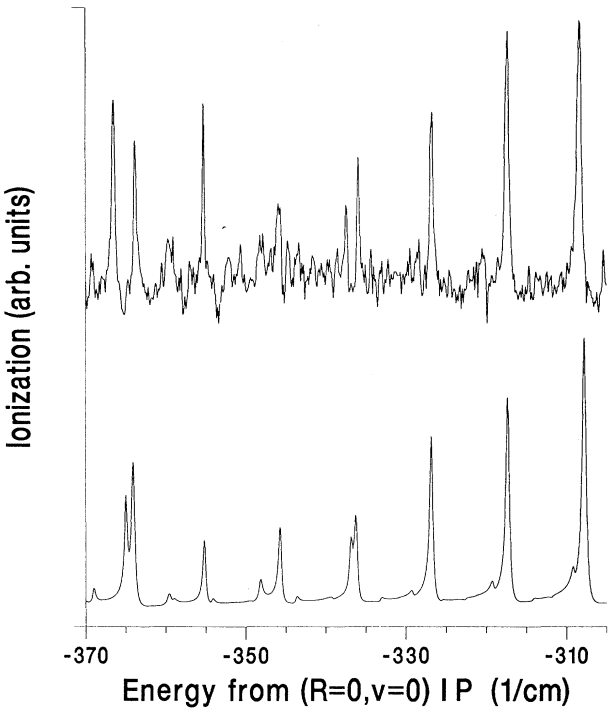

FIG. 7. Comparison between the π-polarization ionization spectrum at 4.32 kV/cm and the results of a single-channel QDT-Stark calculation as described in the text. The experimental spectrum is at the top.

Due to the nonuniformities in our electric field, the residual Doppler width in the transitions to the Stark states, and our finite laser linewidths, we are generally unable to resolve the actual line shapes of the Stark resonances. Thus we lose details of the Stark spectra such as asymmetries in the lines and interference dips. Future work at higher resolution may resolve the line shapes of individual Stark components and make an even more detailed comparison between theory and experiment possible.

A very interesting dynamic behavior is observable near the crossing of the (19,−6) and (17,8) states, as well as at several other crossings in the region well above E_c. This can be seen in Figs. 5 and 6 which plot the ionization and dissociation Stark maps in the energy region around this crossing. Over most of this region there is very little dissociation yield from the states involved in the crossing; however, in a narrow range of field centered roughly 100 V/cm above the field at which the crossing occurs (4.4 kV/cm), the dissociation yield for the state on the high-energy side of the crossing becomes large. There are several possible explanations for this dynamic behavior. One is that there may be an unseen predissociated perturbing state near this energy that mixes with the Stark state and induces strong predissociation in it over a narrow range of energies. We view this as unlikely, since there is no known perturber at this energy and other Stark states which cross this energy do not show a similar behavior. The other possibility, which we view as more likely, is that there is an interference-induced cancellation of the ionization rate near the crossing. Such cancellations can significantly reduce the ionization rate of a state over a narrow range of field; were such a reduction to occur, dissociation would become the dominant decay mechanism for the Stark state over this field range. Attempts to model the ionization behavior of the states near this crossing using single-channel theory have failed; although the theory predicts an interference cancellation in this region, it is for the wrong state and at the wrong field. This is to be expected if the theory is not correctly predicting the strength of the coupling between the states due to the presence of additional rotational coupling. Again, the single-channel theory fails to quantitatively

reproduce the experimental observations near crossings, indicating the need for explicit inclusion of different core rotational channels in a multichannel calculation.

CONCLUSION

We have generated Stark maps of H_2 Rydberg states which simultaneously measure relative ionization and dissociation yields. The energies of the highly excited Stark states are approximately in agreement with the predictions of fourth-order hydrogenic perturbation theory and a single-channel QDT-Stark calculation; however, the couplings between Stark states predicted by the single-channel calculation are considerably too small, indicating that the coupling between states converging to different ionic core levels must be included. The general dynamic behavior of the excited states can be understood using simple arguments based on the known behavior of Stark Rydberg states of complex systems.

Our results show that a detailed understanding of the Stark effect in this simplest of molecular systems will require the application of multichannel treatments, including rotational and perhaps vibrational interactions. We are in the process of developing such a theoretical treatment, based on the work of Harmin [27] and Jungen [21]. We also plan to make higher-resolution measurements with the aim of resolving the Stark resonance line shapes.

ACKNOWLEDGMENTS

This work was supported by the Robert A. Welch Foundation through Grant No. D-1204, and the Research Enhancement Fund of the Graduate School of Texas Tech University. The authors wish to thank Dr. Thomas Bergeman of SUNY–Stony Brook for many illuminating discussions and his willingness to perform single-channel QDT-Stark calculations and for supplying us with the single-channel codes.

[1] D. A. Harmin, Phys. Rev. A **26**, 2656 (1982); L. DiMauro, T. Bergeman, P. McNicholl, and H. Metcalf, J. Phys. (Paris) Colloq. **43**, C2-167 (1982); D. J. Armstrong, C. H. Greene, R. P. Wood, and J. Cooper, Phys. Rev. Lett. **70**, 2379 (1993).
[2] K. Sakimoto, J. Phys. B **22**, 2727 (1989).
[3] W. L. Glab and J. P. Hessler, Phys. Rev. A **42**, 5486 (1990).
[4] J. Chevaleyre, C. Bordas, M. Broyer, and P. Labastie, Phys. Rev. Lett. **57**, 3027 (1986).
[5] G. R. Janik, O. C. Mullins, C. R. Mahon, and T. F. Gallagher, Phys. Rev. A **35**, 2345 (1987).
[6] C. R. Mahon, G. R. Janik, and T. F. Gallagher, Phys. Rev. A **41**, 3746 (1990).
[7] H. H. Fielding and T. P. Softley, Chem. Phys. Lett. **185**, 199 (1991).
[8] W. L. Glab and K. Qin, J. Chem. Phys. (to be published).
[9] K. Qin, M. Bistransin, and W. L. Glab, Phys. Rev. A **47**, 4154 (1993).
[10] C. Bordas and H. Helm, Phys. Rev. A **47**, 1209 (1993).
[11] W. A. Chupka, J. Chem. Phys. **98**, 4520 1993).
[12] S. T. Pratt, J. Chem. Phys. **98**, 9241 (1993).
[13] W. L. Glab and J. P. Hessler, Phys. Rev. A **35**, 2102 (1987).
[14] W. L. Glab and J. P. Hessler, Appl. Opt. **26**, 3181 (1987).
[15] B. A. Palmer, R. A. Keller, and R. Engelman, Jr., Los Alamos Scientific Laboratory Informal Report No. LA-8251-MS, 1980 (unpublished).
[16] M. L. Zimmerman, M. G. Littman, M. M. Kash, and D. Kleppner, Phys. Rev. A **20**, 2251 (1979).
[17] D. A. Harmin, Phys. Rev. A **30**, 2413 (1984).
[18] H. J. Silverstone, Phys. Rev. A **18**, 1853 (1978).
[19] R. J. Damburg and V. V. Kolosov, J. Phys. B **12**, 2637 (1979).
[20] Luc-Koenig and A. Bachelier, J. Phys. B **13**, 1743 (1980).
[21] Ch. Jungen, Phys. Rev. Lett. **53**, 2394 (1984).
[22] F. J. Comes and U. Wenning, Chem. Phys. Lett. **5**, 195 (1970).
[23] S. Feneuille, S. Liberman, E. Luc-Koenig, J. Pinard, and A. Taleb, J. Phys. B **15**, 1205 (1982).
[24] J. M. Lecomte and E. Luc-Koenig, J. Phys. B **18**, L357 (1985).
[25] P. McNicholl, T. Bergeman, and H. J. Metcalf, Phys. Rev. A **37**, 3302 (1988).
[26] H. Rottke and K. H. Welge, J. Chem. Phys. **97**, 908 (1992).
[27] D. A. Harmin, Comments At. Mol. Phys. **15**, 281 (1985).